

# Sparse Grid Time-Discontinuous Galerkin Method with Streamline Diffusion for Transport Equations

Andreas Zeiser

Version: April 12, 2022 / Received: date / Accepted: date

**Abstract** High-dimensional transport equations frequently occur in science and engineering. Computing their numerical solution, however, is challenging due to its high dimensionality.

In this work we develop an algorithm to efficiently solve the transport equation in moderately complex geometrical domains using a Galerkin method stabilized by streamline diffusion. The ansatz spaces are a tensor product of a sparse grid in space and discontinuous piecewise polynomials in time. Here, the sparse grid is constructed upon nested multilevel finite element spaces to provide geometric flexibility. This results in an implicit time-stepping scheme which we prove to be stable and convergent. If the solution has additional mixed regularity, the convergence of a  $2d$ -dimensional problem equals that of a  $d$ -dimensional one up to logarithmic factors.

For the implementation, we rely on the sparse grid combination technique, which enables us to store the functions and to carry out the computations on a sequence of anisotropic full grids exploiting the tensor product structure of the ansatz spaces. In this way existing finite element libraries and GPU acceleration can be used. The combination technique is also used as a preconditioner for an iterative scheme to solve the transport equation on the sequence of time strips.

Numerical tests show that the method works well for problems in up to six dimensions. Finally, the method is also used as a building block to solve nonlinear Vlasov-Poisson equations.

**Keywords** Sparse grid · High-dimensional transport equations · Streamline diffusion · Combination technique · Vlasov-Poisson equations

**Mathematics Subject Classification (2020)** 65M60 · 65M12

---

A. Zeiser (ORCID 0000-0003-2552-4778)  
Fachbereich 1 Ingenieurwissenschaften – Energie und Information, HTW Berlin, Wilhelminenhofstr. 75  
A, 12459 Berlin, Germany  
E-mail: andreas.zeiser@htw-berlin.de

## 1 Introduction

High-dimensional transport equations frequently arise in science and engineering. In this paper we will consider the linear equation

$$\begin{aligned} \partial_t u + \beta(t, \mathbf{r}) \cdot \nabla_{\mathbf{r}} u + \sigma(t, \mathbf{r}) u &= f(t, \mathbf{r}), \quad \text{in } (0, T) \times \Omega \\ u(0, \mathbf{r}) &= u_0(\mathbf{r}) \end{aligned} \quad (1)$$

subject to the inflow boundary condition

$$u = g \quad \text{on } \Gamma_r^- = \{(t, \mathbf{r}) \in (0, T) \times \partial\Omega \mid \beta(t, \mathbf{r}) \cdot \mathbf{n}(\mathbf{r}) < 0\} \quad (2)$$

where  $\mathbf{n}(\mathbf{r})$  is the outward unit normal of the spatial boundary, and  $\beta, f, \sigma, g, u_0$  are smooth enough functions. We will focus on the case where the variable  $\mathbf{r}$  can be partitioned into  $\mathbf{r} = (\mathbf{x}, \mathbf{v})$  and  $\mathbf{x}, \mathbf{v}$  are  $d$ -dimensional variables with  $d = 1, 2, 3$  (i.e., space and velocity). We assume that  $\Omega$  is a product domain (i.e.,  $\Omega = \Omega^{(1)} \times \Omega^{(2)}$  with  $\Omega^{(1)}, \Omega^{(2)} \subset \mathbb{R}^d$ ).

Simulations of such systems are computationally demanding since the time evolution of an up to six-dimensional function has to be calculated. Applying standard discretization schemes leads to an evolution equation in  $\mathcal{O}(n^{2d})$  degrees of freedom, where  $n$  is the number of grid points in one dimension and a corresponding high computational effort. To tackle the problem, methods such as particle methods [23], adaptive multiscale methods [2, 4] and tensor product methods [5] have been used.

Sparse grids [3] are a means of overcoming the curse of dimensionality and have been applied to transport equations [21] as well as to kinetic equations: in [17] interpolation on sparse grids is used in a semi-Lagrangian method while [12] uses sparse grids with discontinuous ansatz functions. In these approaches tensor products of one-dimensional bases are used, restricting the domain to rectangular regions. However, finite element spaces can also be used in the construction of sparse grid spaces [7, 13] allowing for greater geometric flexibility. Such bases were already applied in the context of radiative transfer [25].

Our aim is to use such sparse grid spaces based upon finite element spaces to devise a stable, convergent and efficient method for the solution of kinetic equations in moderately complex geometrical domains. We also focus on their efficient implementation using well-established finite element libraries and fast algorithms.

For that purpose, we will use the streamline diffusion method [15] and a discontinuous time discretization resulting in an implicit time-stepping scheme. The sparse grid combination technique (see [6] and references therein) will enable us to carry out the computations on a sequence of anisotropic full grids and use the tensor product structure of the ansatz spaces. Moreover, it will also serve as a preconditioner for the iterative solution of the corresponding equations.

We will proceed along the following lines. In Sect. 2 sparse grid spaces are introduced, and the weak form, including streamline diffusion, is employed to derive discrete equations for each time step. This algorithm is analyzed in Sect. 3 in the case of constant coefficients with respect to stability and convergence. Sect. 4 describes the algorithm for efficient computations based on the tensor product structure and multilevel spaces. The algorithm is applied to test cases in Sect. 5 as well as to Vlasov-Poisson equations in one and two spatial dimensions.

## 2 Discretization and Weak Formulation

In this section we introduce the weak formulation of the transport problem including streamline diffusion [15] for stabilization. For the discretization we will use a sparse grid based on finite elements and discontinuous polynomials in time. Finite element spaces have been used in the construction of sparse grids, realized either by wavelet-type [22, 25] or multilevel frames [13]. We will use the latter approach and use the combination technique described in [8]. This enables us to use classical nested finite element spaces. We partition the time domain, use discontinuous piecewise polynomials and a full tensor product with the sparse grid, see [14] in the case of parabolic equations. Eventually this will lead us to an implicit time-stepping scheme.

Let  $\Omega^{(1)}$  and  $\Omega^{(2)}$  be two open polyhedral Lipschitz domains in  $d$  space dimensions and  $V_1^{(i)}$  conforming finite element spaces on  $\Omega^{(i)}$ . Define nested multilevel finite element spaces

$$V_1^{(i)} \subset V_2^{(i)} \subset \dots \subset H^1(\Omega^{(i)}), \quad i = 1, 2$$

by uniform refinement. Based on these spaces the sparse tensor product space of level  $L = 1, 2, \dots$

$$V_L = \sum_{|\ell|_1 \leq L+1} V_{\ell_1}^{(1)} \otimes V_{\ell_2}^{(2)}, \quad \ell = [\ell_1, \ell_2], \quad |\ell|_1 = \ell_1 + \ell_2 \quad (3)$$

is constructed with  $\dim V_L \lesssim L2^{dL}$  [8]. Up to a logarithmic factor the number of degrees of freedom scales like a standard globally refined finite element discretization of a  $d$ -dimensional domain.

In the time domain  $J = (0, T)$  define  $0 = t_0 < t_1 < \dots < t_N = T$  and the partition

$$\mathcal{J} = \{I_j\}_{j=1, \dots, N}, \quad I_j = (t_{j-1}, t_j), \quad |\mathcal{J}| = \max_{j=1, \dots, N} (t_j - t_{j-1}).$$

The discrete function space is defined as the set of all piecewise polynomials of order  $r$  with coefficients in  $V_L$ , i.e.

$$V_{L, \mathcal{J}} = \{v \in L^2(J; V_L) \mid v|_I \in \mathbb{P}^r(I; V_L) \text{ for all } I \in \mathcal{J}\},$$

where  $\mathbb{P}^r$  denotes the polynomials degree  $r$ .

We will use the space  $V_{L, \mathcal{J}}$  to compute an approximate solution of (1) and (2). For that purpose, we use the streamline diffusion method on each time strip  $I_j$  [15]. The initial condition and the inflow condition are enforced in a weak sense:

For  $j = 1, 2, \dots, N$  find a function  $U_j \in \mathbb{P}^r(I_j, V_L)$  on the time strip  $I_j \in \mathcal{J}$ ,  $j = 1, \dots, N$ , such that

$$a_j^{(\delta)}(U_j, w) = b_j^{(\delta)}(w), \quad \text{for all } w \in \mathbb{P}^r(I_j, V_L) \quad (4)$$

where  $\delta > 0$  is the parameter for the streamline diffusion and

$$\begin{aligned} a_j^{(\delta)}(U, w) &= \int_{I_j} (\partial_t U + \partial_\beta U + \sigma U, w + \delta(\partial_t w + \partial_\beta w)) - \langle U, w \rangle_{\hat{\Gamma}^-(t)} dt \\ &\quad + (U_{j-1}^+, w_{j-1}^+) \\ b_j^{(\delta)}(w) &= \int_{I_j} (f, w + \delta(\partial_t w + \partial_\beta w)) - \langle g, w \rangle_{\hat{\Gamma}^-(t)} dt + (U_{j-1}^-, w_{j-1}^+). \end{aligned}$$

Here  $\partial_\beta u = \beta \cdot \nabla u$ ,  $u_j^\pm = \lim_{t \rightarrow t_j^\pm} u(t, \cdot)$ ,  $U_0^- = u_0$ . By  $(\cdot, \cdot)$  and  $\|\cdot\|$  denote the inner product and norm on  $L^2(\Omega)$ , respectively. For the boundary define

$$\hat{\Gamma}^\pm(t) = \{\mathbf{r} \in \partial\Omega \mid \beta(\mathbf{r}, t) \cdot \mathbf{n}(\mathbf{r}) \gtrless 0\}$$

and for any  $\hat{\Gamma} \subset \partial\Omega$

$$\langle u, v \rangle_{\hat{\Gamma}} = \int_{\hat{\Gamma}} (\beta \cdot \mathbf{n}) uv ds, \quad |u|_{\hat{\Gamma}}^2 = \int_{\hat{\Gamma}} |\beta \cdot \mathbf{n}| u^2 ds.$$

Equation (4) can be solved successively, resulting in an implicit time-stepping procedure. Finally, the approximate solution  $U \in V_{L, \mathcal{J}}$  is composed of the solutions  $U_j$  with potential jumps at  $t_j$ .

### 3 Analysis – Constant Coefficients

In this section the stability and convergence of the discretization is analyzed for the case of constant coefficients. Hence, for the rest of this section we assume  $\beta \in \mathbb{R}^{2d}$ ,  $\sigma \geq 0$ ,  $f \in L^2(J \times \Omega)$  and  $g \in L^2(J \times \hat{\Gamma}^-)$ . A similar analysis for stationary transport dominated problems has been carried out in [21] and for parabolic equations in [14]. For an introduction to discontinuous time-stepping schemes and finite element spaces see [18].

For the analysis we formulate the problem on the space  $V_{L, \mathcal{J}}$  by summing up (4) for  $j = 1, \dots, N$ . This gives

$$A_{\mathcal{J}}^{(\delta)}(U, w) = B_{\mathcal{J}}^{(\delta)}(u_0, f, g; w) \quad \text{for all } w \in V_{L, \mathcal{J}}, \quad (5)$$

where

$$\begin{aligned} A_{\mathcal{J}}^{(\delta)}(v, w) &= \sum_{j=1}^N \int_{I_j} (\partial_t v + \partial_\beta v + \sigma v, w + \delta(\partial_t w + \partial_\beta w)) - \langle v, w \rangle_{\hat{\Gamma}^-} dt \\ &\quad + \sum_{j=1}^{N-1} ([v]_j, w_j^+) + (v_0^+, w_0^+) \end{aligned} \quad (6)$$

$$B_{\mathcal{J}}^{(\delta)}(u_0, f, g; w) = \sum_{j=1}^N \int_{I_j} (f, w + \delta(\partial_t w + \partial_\beta w)) - \langle g, w \rangle_{\hat{\Gamma}^-} dt + (u_0, w_0^+) \quad (7)$$

with the jump term  $[v]_j = v_j^+ - v_j^-$ . Note that the boundaries  $\hat{\Gamma}^\pm$  are now time independent.

For the analysis the streamline diffusion norm

$$\|u\|_\delta^2 = \sum_{j=1}^N \int_{I_j} \sigma \|v\|^2 + \delta \|\partial_t v + \partial_\beta v\|^2 + |v|_{\partial\Omega}^2 dt + \sum_{j=1}^{N-1} \|[v]_j\|^2 + \|v_0^+\|^2 + \|v_N^-\|^2 \quad (8)$$

will play a central role. This norm gives extra control of the variations in the direction of the streamline.

### 3.1 Stability

In the first step we show that the method is stable with respect to the streamline diffusion norm. The following equivalence plays a central role.

**Lemma 1** *Let  $v \in H^1(J \times \Omega)$ ,  $\sigma \geq 0$ ,  $0 < \delta$  and  $\delta < 1/\sigma$  in the case  $\sigma > 0$ . Then*

$$\frac{1}{2} \|v\|_\delta^2 \leq A_{\mathcal{J}}^{(\delta)}(v, v) \leq \frac{3}{2} \|v\|_\delta^2. \quad (9)$$

*Proof* Applying Green's identity

$$\begin{aligned} \int_{I_j} (\partial_t v, w) dt &= (v_j^-, w_j^-) - (v_{j-1}^+, w_{j-1}^+) - \int_{I_j} (v, \partial_t w) dt \\ \int_{I_j} (\partial_\beta v, w) dt &= \int_{I_j} \langle v, w \rangle_{\partial\Omega} - (v, \partial_\beta w) dt \end{aligned}$$

on (6) gives

$$\begin{aligned} A_{\mathcal{J}}^{(\delta)}(v, w) &= \sum_{j=1}^N \int_{I_j} (-v, \partial_t w + \partial_\beta w) + (\sigma v, w + \delta(\partial_t w + \partial_\beta w)) dt \\ &\quad + \sum_{j=1}^N \int_{I_j} \delta(\partial_t v + \partial_\beta v, \partial_t w + \partial_\beta w) + \langle v, w \rangle_{\hat{\Gamma}^+} dt \\ &\quad + \sum_{j=1}^{N-1} (v_j^-, -[w]_j) + (v_N^-, w_N^-). \end{aligned} \quad (10)$$

Averaging the two forms for  $A_{\mathcal{J}}^{(\delta)}(v, v)$  gives

$$\begin{aligned} A_{\mathcal{J}}^{(\delta)}(v, v) &= \sum_{j=1}^N \int_{I_j} \sigma \|v\|^2 + \frac{1}{2} |v|_{\partial\Omega}^2 + \delta \|\partial_t v + \partial_\beta v\|^2 dt \\ &\quad + \sum_{j=1}^N \int_{I_j} \delta \sigma (v, \partial_t v + \partial_\beta v) dt + \frac{1}{2} \sum_{j=1}^{N-1} \|[v]_j\|^2 + \frac{1}{2} \|v_0^+\|^2 + \frac{1}{2} \|v_N^-\|^2. \end{aligned} \quad (11)$$

For  $\sigma > 0$  the second term can be estimated by

$$\left| \sum_{j=1}^N \int_{I_j} \delta \sigma (v, \partial_t v + \partial_\beta v) dt \right| \leq \sum_{j=1}^N \int_{I_j} \frac{\delta \sigma^2}{2} \|v\|^2 + \frac{\delta}{2} \|\partial_t v + \partial_\beta v\|^2 dt.$$

Using  $\delta < 1/\sigma$ , the equivalence follows directly using the definition of the streamline diffusion norm (8).  $\square$

Now we use the Lemma to prove stability.

**Theorem 1** *If  $\delta > 0$  is small enough, the weak form of the streamline diffusion equation with constant coefficients (5) has a unique solution  $U$ . If  $\sigma > 0$  the system is stable in the sense that the solution satisfies*

$$\|U\|_\delta^2 \lesssim \sum_{j=1}^N \int_{I_j} \|f\|^2 + |g|_{\tilde{\Gamma}^-}^2 dt + \|u_0\|^2.$$

For the case  $\sigma = 0$  a similar bound can be derived where however the constant depends exponentially on the final time  $T$ .

*Proof* For  $\sigma > 0$  applying Cauchy and Young's inequality on (7) gives

$$\begin{aligned} B^{(\delta)}(u_0, f, g; v) &\leq \sum_{j=1}^N \int_{I_j} \left( \frac{1}{\sigma} + \delta \right) \|f\|^2 + \frac{\sigma}{4} \|v\|^2 + \frac{\delta}{4} \|\partial_t v + \partial_\beta v\|^2 + |g|_{\tilde{\Gamma}^-}^2 + \frac{1}{4} |v|_{\tilde{\Gamma}^-}^2 dt \\ &\quad + \|u_0\|^2 + \frac{1}{4} \|v_0^+\|^2 \\ &\leq \frac{1}{2} A_{\mathcal{J}}^{(\delta)}(v, v) + \sum_{j=1}^N \int_{I_j} \left( \frac{1}{\sigma} + \delta \right) \|f\|^2 + |g|_{\tilde{\Gamma}^-}^2 dt + \|u_0\|^2, \end{aligned}$$

where Lemma 1 was used in the last step. The solution  $U$  satisfies

$$\begin{aligned} A_{\mathcal{J}}^{(\delta)}(U, U) &= B_{\mathcal{J}}^{(\delta)}(u_0, f, g; U) \\ &\leq \frac{1}{2} A_{\mathcal{J}}^{(\delta)}(U, U) + \sum_{j=1}^N \int_{I_j} \left( \frac{1}{\sigma} + \delta \right) \|f\|^2 + |g|_{\tilde{\Gamma}^-}^2 dt + \|u_0\|^2. \end{aligned}$$

Bringing  $A_{\mathcal{J}}^{(\delta)}(U, U)$  to the left side and using (9) gives the inequality which also shows the existence and uniqueness of the solution.

For the case  $\sigma = 0$  one can introduce a positive constant term by change of the unknown to  $w(t, \cdot) = e^{-\alpha t} u(t, \cdot)$  which leads to an exponential factor  $e^{\alpha T}$  in the bound [15].  $\square$

### 3.2 Approximation

In the following we will derive error estimates for the orthogonal projection onto  $V_{L,\mathcal{J}}$ , which will be used in the convergence proof in Sect. 3.3. For the result we will combine estimates for sparse grids and well known approximation results from one-dimensional finite element discretizations for the time domain.

Following [8] we assume that the approximation property

$$\inf_{v_\ell \in V_\ell^{(i)}} \|u - v_\ell\|_{H^q(\Omega^{(i)})} \lesssim h_\ell^{s-q} \|u\|_{H^s(\Omega^{(i)})}, \quad u \in H^s(\Omega^{(i)}), \quad i = 1, 2$$

holds for  $q < \gamma$ ,  $q \leq s \leq r + 1$  uniformly in the level  $\ell$  (note that we replaced  $r$  by  $r + 1$ ). Here  $h_\ell = 2^{-\ell}$  and

$$\gamma = \sup \{s \in \mathbb{R} \mid V_\ell^{(1)} \subset H^s(\Omega^{(1)}), V_\ell^{(2)} \subset H^s(\Omega^{(2)})\}.$$

Define for  $s > 0$  the Sobolev spaces of mixed order [10]

$$H_{\text{mix}}^s(\Omega) = H_{\text{mix}}^{s,s}(\Omega), \quad H_{\text{mix}}^{s_1,s_2}(\Omega) = H^{s_1}(\Omega^{(1)}) \otimes H^{s_2}(\Omega^{(2)})$$

and denote the corresponding norm by  $\|\cdot\|_{H_{\text{mix}}^s}$ . Then the following approximation results hold.

**Theorem 2 ([8])** *Let  $0 < s \leq r$  and denote by  $P_L$  the  $L^2$ -orthogonal projection onto  $V_L$ . Then*

$$\begin{aligned} \|u - P_L u\|_{L^2(\Omega)} &\lesssim 2^{-(s+1)L} \sqrt{L} \|u\|_{H_{\text{mix}}^{s+1}(\Omega)} \\ \|u - P_L u\|_{H^1(\Omega)} &\lesssim 2^{-sL} \sqrt{L} \|u\|_{H_{\text{mix}}^{s+1}(\Omega)} \end{aligned}$$

if  $u \in H_{\text{mix}}^{s+1}(\Omega)$ .

*Proof* The inequalities directly follow from [8, Thm. 1] for the case  $n_1 = n_2 = d$ ,  $\sigma = 1$ , and Examples 1 and 2.  $\square$

Finally, define the space

$$\mathcal{H}^s(J \times \Omega) = H^s(J) \otimes L^2(\Omega) \cap L^2(J) \otimes H_{\text{mix}}^s(\Omega)$$

with classical regularity with respect to time and a mixed regularity with respect to  $\mathbf{x}$  and  $\mathbf{v}$ . The corresponding norm reads

$$\|u\|_{\mathcal{H}^s}^2 = \int_0^T \|\partial_t^s u\|_{L^2(\Omega)}^2 + \|u\|_{H_{\text{mix}}^s(\Omega)}^2 dt.$$

With this type of regularity we can show the following approximation result.

**Theorem 3** Let  $L \in \mathbb{N}$  and let  $\mathcal{J}$  be a time partition such that  $|\mathcal{J}| \sim h = 2^{-L}$ . For  $u \in L^2(J \times \Omega)$  define

$$u_h = (P_{\mathcal{J}} \otimes P_L)u,$$

where  $P_{\mathcal{J}}$  is the  $L^2$ -orthogonal projection onto the continuous piecewise polynomials of degree  $r$  with respect to the partition  $\mathcal{J}$ . For  $0 < s \leq r$  and  $u \in \mathcal{H}^{s+1}$

$$\begin{aligned} \|u - u_h\|_{L^2(J \times \Omega)} &\lesssim 2^{-(s+1)L} \sqrt{L} \|u\|_{\mathcal{H}^{s+1}} \sim h^{s+1} (\ln h)^{1/2} \|u\|_{\mathcal{H}^{s+1}}, \\ \|u - u_h\|_{H^1(J \times \Omega)} &\lesssim 2^{-sL} \sqrt{L} \|u\|_{\mathcal{H}^{s+1}} \sim h^s (\ln h)^{1/2} \|u\|_{\mathcal{H}^{s+1}}, \end{aligned}$$

where the constants are independent of  $L$  and  $u$ .

*Proof* For  $v \in H^{s+1}(J)$  the operator  $P_{\mathcal{J}}$  satisfies

$$\|v - P_{\mathcal{J}}v\|_{L^2(J)} \lesssim |\mathcal{J}|^{s+1} \|\partial_t^{s+1} v\|_{L^2(J)}, \quad \|v - P_{\mathcal{J}}v\|_{H^1(J)} \lesssim |\mathcal{J}|^s \|\partial_t^{s+1} v\|_{L^2(J)}.$$

The projection error with respect to  $L^2$  can be estimated by

$$\begin{aligned} \|u - u_h\|_{L^2(J \times \Omega)} &= \|(I - P_{\mathcal{J}}) \otimes P_L u + P_{\mathcal{J}} \otimes (I - P_L) u + (I - P_{\mathcal{J}}) \otimes (I - P_L) u\|_{L^2(J \times \Omega)} \\ &\leq \|I - P_{\mathcal{J}}\|_{H^{s+1}(J) \rightarrow L^2(J)} \|P_L\|_{L^2(\Omega) \rightarrow L^2(\Omega)} \|u\|_{H^{s+1}(J) \otimes L^2(\Omega)} \\ &\quad + \|P_{\mathcal{J}}\|_{L^2(J) \rightarrow L^2(J)} \|I - P_L\|_{H_{\text{mix}}^{s+1}(\Omega) \rightarrow L^2(\Omega)} \|u\|_{L^2(J) \otimes H_{\text{mix}}^{s+1}(\Omega)} \\ &\quad + \|I - P_{\mathcal{J}}\|_{H^{s+1}(J) \rightarrow L^2(J)} \|I - P_L\|_{L^2(\Omega) \rightarrow L^2(\Omega)} \|u\|_{H^{s+1}(J) \otimes L^2(\Omega)} \\ &\lesssim 2^{-(s+1)L} \sqrt{L} \|u\|_{\mathcal{H}^{s+1}}. \end{aligned}$$

For the second inequality note that

$$H^1(J \times \Omega) = H^1(J) \otimes L^2(\Omega) \cap L^2(J) \otimes H_{\text{mix}}^{1,0}(\Omega) \cap L^2(J) \otimes H_{\text{mix}}^{0,1}(\Omega)$$

We estimate each contribution like in the previous case:

$$\begin{aligned} \|u - u_h\|_{H^1(J) \otimes L^2(\Omega)} &\leq \|I - P_{\mathcal{J}}\|_{H^{s+1}(J) \rightarrow H^1(J)} \|P_L\|_{L^2(\Omega) \rightarrow L^2(\Omega)} \|u\|_{H^{s+1}(J) \otimes L^2(\Omega)} \\ &\quad + \|P_{\mathcal{J}}\|_{L^2(J) \rightarrow H^1(J)} \|I - P_L\|_{H_{\text{mix}}^{s+1}(\Omega) \rightarrow L^2(\Omega)} \|u\|_{L^2(J) \otimes H_{\text{mix}}^{s+1}(\Omega)} \\ &\quad + \|I - P_{\mathcal{J}}\|_{H^{s+1}(J) \rightarrow H^1(J)} \|I - P_L\|_{L^2(\Omega) \rightarrow L^2(\Omega)} \|u\|_{H^{s+1}(J) \otimes L^2(\Omega)} \end{aligned}$$

and use the inverse inequality of  $P_{\mathcal{J}}$  to bound  $\|P_{\mathcal{J}}\|_{L^2(J) \rightarrow H^1(J)} \lesssim |\mathcal{J}|^{-1} \sim 2^L$  which leads to

$$\|u - u_h\|_{H^1(J) \otimes L^2(\Omega)} \lesssim 2^{-sL} \sqrt{L} \|u\|_{\mathcal{H}^{s+1}}.$$



In the same manner

$$\begin{aligned}
& \|u - u_h\|_{L^2(J) \otimes H_{\text{mix}}^{1,0}(\Omega)} \\
& \leq \| (I - P_{\mathcal{J}}) \|_{H^{s+1}(J) \rightarrow L^2(J)} \|P_L\|_{L^2(\Omega) \rightarrow H_{\text{mix}}^{1,0}(\Omega)} \|u\|_{H^{s+1}(J) \otimes L^2(\Omega)} \\
& \quad + \|P_{\mathcal{J}}\|_{L^2(J) \rightarrow L^2(J)} \|I - P_L\|_{H_{\text{mix}}^{s+1}(\Omega) \rightarrow H^1(\Omega)} \|u\|_{L^2(J) \otimes H_{\text{mix}}^{s+1}(\Omega)} \\
& \quad + \|I - P_{\mathcal{J}}\|_{L^2(J) \rightarrow L^2(J)} \|I - P_L\|_{H_{\text{mix}}^{s+1}(\Omega) \rightarrow H_{\text{mix}}^{1,0}(\Omega)} \|u\|_{L^2(J) \otimes H_{\text{mix}}^{s+1}(\Omega)} \\
& \lesssim 2^{-sL} \sqrt{L} \|u\|_{\mathcal{H}^{s+1}}.
\end{aligned}$$

Here we use the inverse inequality  $\|P_L\|_{L^2(\Omega) \rightarrow H^1(\Omega)} \lesssim 2^L$ . The last norm with respect to  $L^2(J) \otimes H_{\text{mix}}^{0,1}(\Omega)$  is treated analogously. Summing up all contributions proves the second inequality.  $\square$

### 3.3 Convergence

Using the approximation result from the previous section we can prove the convergence of the discrete solution.

**Theorem 4** *Let  $u$  be a solution of the transport problem (1) and (2) in the case of constant coefficients and  $\sigma \geq 0$  and assume that  $u \in \mathcal{H}^{s+1}$  for  $0 < s \leq r$ . Let  $U$  be the solution of the discrete equations (5) for level  $L$ , where  $|\mathcal{J}| \sim h = 2^{-L}$  and  $\delta \sim h$  small enough. Then*

$$\|U - u\|_{\delta} \lesssim h^{s+1/2} (\ln h)^{1/2} \|u\|_{\mathcal{H}^{s+1}}.$$

*Proof* The proof follows along the lines of [18, Thm 13.7] and [21]. Decompose the error

$$e = U - u = (U - \tilde{u}) + (\tilde{u} - u) = \theta + \rho, \quad \tilde{u} = (P_{\mathcal{J}} \otimes P_L)u.$$

The streamline diffusion norm can be estimated by

$$\|e\|_{\delta} \leq \|\theta\|_{\delta} + \|\rho\|_{\delta}. \quad (12)$$

For the first term note that

$$\|\theta\|_{\delta}^2 \lesssim A_{\mathcal{J}}^{(\delta)}(\theta, \theta) = -A_{\mathcal{J}}^{(\delta)}(\rho, \theta),$$

where the Galerkin orthogonality has been used. Applying (10) for the right hand side, using Young's inequality and Lemma 1 gives the estimate

$$\begin{aligned}
& |A_{\mathcal{J}}^{(\delta)}(\rho, \theta)| \\
& \leq \sum_{j=1}^N \int_{I_j} 2\delta^{-1} \|\rho\|^2 + \frac{\delta}{8} \|\partial_t \theta + \partial_\beta \theta\|^2 + \sigma \|\rho\|^2 + \frac{\sigma}{4} \|\theta\|^2 + |\rho|_{\tilde{\Gamma}^+}^2 + \frac{1}{4} |\theta|_{\tilde{\Gamma}^+}^2 \\
& \quad + 2\delta \|\partial_t \rho + \partial_\beta \rho\|^2 + \frac{\delta}{8} \|\partial_t \theta + \partial_\beta \theta\|^2 + 2\delta \sigma^2 \|\rho\|^2 + \frac{\delta}{8} \|\partial_t \theta + \partial_\beta \theta\|^2 dt \\
& \quad + \sum_{j=1}^N \|\rho_j\|^2 + \frac{1}{4} \sum_{j=1}^{N-1} \|[\theta]_j\|^2 + \frac{1}{4} \|\theta_N^-\|^2 \\
& \leq \frac{1}{2} A_{\mathcal{J}}^{(\delta)}(\theta, \theta) \\
& \quad + C \left[ \sum_{j=1}^N \int_{I_j} (1 + \delta^{-1}) \|\rho\|^2 + \delta \|\partial_t \rho + \partial_\beta \rho\|^2 + |\rho|_{\tilde{\Gamma}^+}^2 dt + \sum_{j=1}^N \|\rho_j\|^2 \right].
\end{aligned}$$

Here we used the fact that  $\rho$  is continuous in time. Hence it follows that

$$\|\theta\|_\delta^2 \lesssim \sum_{j=1}^N \int_{I_j} (1 + \delta^{-1}) \|\rho\|^2 + \delta \|\partial_t \rho + \partial_\beta \rho\|^2 + |\rho|_{\tilde{\Gamma}^+}^2 dt + \sum_{j=1}^N \|\rho_j\|^2.$$

For the second term in (12)

$$\|\rho\|_\delta^2 \lesssim \sum_{j=1}^N \int_{I_j} \|\rho\|^2 + \delta \|\partial_t \rho + \partial_\beta \rho\|^2 + |\rho|_{\partial\Omega}^2 dt + \|\rho_0\|^2 + \|\rho_N\|^2,$$

where again the continuity of  $\rho$  was used. Applying the trace inequality on each strip  $I_j \times \Omega$  gives

$$\begin{aligned}
\|\rho_{j-1}\|^2 + \|\rho_j\|^2 + \int_{I_j} |\rho|_{\partial\Omega}^2 dt & \lesssim \|\rho\|_{L^2(I_j \times \Omega)} \cdot \|\rho\|_{H^1(I_j \times \Omega)} \\
& \lesssim \delta^{-1} \|\rho\|_{L^2(I_j \times \Omega)}^2 + \delta \|\rho\|_{H^1(I_j \times \Omega)}^2.
\end{aligned}$$

Using

$$\int_{I_j} \|\partial_t \rho + \partial_\beta \rho\|^2 dt \lesssim \|\rho\|_{H^1(I_j \times \Omega)}^2,$$

summing up and applying Thm 3 gives

$$\|e\|_\delta^2 \lesssim (1 + \delta^{-1}) \|\rho\|_{L^2(J \times \Omega)}^2 + \delta \|\rho\|_{H^1(J \times \Omega)}^2 \lesssim h_L^{2s+1} \ln h_L \|u\|_{\mathcal{H}^{s+1}}^2$$

which completes the proof.  $\square$

## 4 Numerical Algorithm

In this section we describe how the discrete equation (4) on each time strip  $I_j$ ,  $j = 1, \dots, N$  is solved. Now we allow the coefficients  $\beta$ ,  $\sigma$  to be functions with sufficient regularity. The aim is to use data structures which enable the efficient representation of the sparse grid functions as well as efficient calculations. For that purpose, we use standard finite element libraries and exploit the tensor product structure of the problem. Therefore we will concentrate on coefficient functions which exhibit a tensor product structure.

### 4.1 Sparse Grid Representation

Traditionally sparse grid spaces are built on multilevel decomposition and require special basis functions resulting in quite sophisticated operations in Galerkin schemes. This problem can be overcome by using the sparse grid combination technique introduced in [11], see also [6]. For sparse grids based on finite element spaces this approach has been used in [8, 13], for example. As a consequence, computations can be carried out on a set of anisotropic full grid tensor product spaces.

It is based on the observation that the space  $V_L$  of (3) can be represented by

$$V_L = \sum_{|\ell|_1=L+1} V_{\ell_1}^{(1)} \otimes V_{\ell_2}^{(2)},$$

i.e. only by those full grid spaces with level  $|\ell|_1 = L + 1$ . However, this is not a direct sum. For representing a function we use the finite element basis

$$V_\ell^{(i)} = \text{span} \{ \varphi_{\ell,k}^{(i)} \mid k = 1, \dots, n_\ell^{(i)} \}, \quad n_\ell^{(i)} = \dim V_\ell^{(i)}$$

for  $i = 1, 2$  and a basis for the polynomials on  $I_j$ :

$$\mathbb{P}^r(I_j, \mathbb{R}) = \text{span} \{ \eta_s^{(j)} \mid s = 0, \dots, r \}.$$

For notational simplicity we will omit the index  $j$  in the following.

Hence a function  $U \in \mathbb{P}^r(I_j, V_L)$  can be written as

$$U(t, \mathbf{x}, \mathbf{v}) = \sum_{|\ell|_1=L+1} \sum_{\substack{0 \leq s \leq r \\ \mathbf{k} \leq \mathbf{n}_\ell}} u_{s,\mathbf{k}}^{(\ell)} \eta_s(t) \varphi_{\ell_1,k_1}^{(1)}(\mathbf{x}) \varphi_{\ell_2,k_2}^{(2)}(\mathbf{v}), \quad \mathbf{n}_\ell = [n_{\ell_1}^{(1)}, n_{\ell_2}^{(2)}].$$

The representation however is not unique since the functions

$$\eta_s \otimes \varphi_{\ell_1,k_1}^{(1)} \otimes \varphi_{\ell_2,k_2}^{(2)}, \quad 0 \leq s \leq r, \mathbf{k} \leq \mathbf{n}_\ell, |\ell|_1 = L + 1, \quad (13)$$

are just a spanning set and not a basis. This leads to additional degrees of freedom, which are negligible for the interesting case of  $d = 2, 3$ , however.

## 4.2 Discrete Equations and Matrices

We will now use the spanning set (13) to derive a system of linear equations for the discrete equation (4) in weak form for a time strip  $I_j$ . Omitting again the index  $j$  gives

$$A^{(\delta)} \mathbf{u} = \mathbf{b}^{(\delta)}, \quad \mathbf{u} = [\mathbf{u}_\ell]_{|\ell|_1=L+1}, \quad \mathbf{u}_\ell = [u_{s,\mathbf{k}}^{(\ell)}]_{\substack{0 \leq s \leq r \\ \mathbf{k}_i \leq n_\ell}} \quad (14)$$

where the blocks are given by

$$A_{\ell,\ell'}^{(\delta)} = \left[ a_j^{(\delta)} (\eta_{s'} \otimes \varphi_{\ell'_1, \mathbf{k}'_1}^{(1)} \otimes \varphi_{\ell'_2, \mathbf{k}'_2}^{(2)}, \eta_s \otimes \varphi_{\ell_1, \mathbf{k}_1}^{(1)} \otimes \varphi_{\ell_2, \mathbf{k}_2}^{(2)}) \right]_{\substack{0 \leq s, s' \leq r \\ \mathbf{k} \leq n_\ell, \mathbf{k}' \leq n_{\ell'}}}$$

$$\mathbf{b}_\ell^{(\delta)} = \left[ b_j^{(\delta)} (\eta_s \otimes \varphi_{\ell_1, \mathbf{k}_1}^{(1)} \otimes \varphi_{\ell_2, \mathbf{k}_2}^{(2)}) \right]_{\substack{0 \leq s \leq r \\ \mathbf{k} \leq n_\ell}}$$

for  $|\ell|_1, |\ell'|_1 = L+1$ . Note that the matrix  $A^{(\delta)}$  is not invertible, but the system is still solvable since the right hand side is in the range of the matrix [9]. We will later use iterative methods to solve the system which are based on the application of the matrix to a vector, see Sect. 4.3.

For its efficient calculation we exploit the tensor product structure for each individual block  $A_{\ell,\ell'}^{(\delta)}$ . In the first step we use a quadrature rule of sufficient order for the time integration on the interval  $I_j = [t_{j-1}, t_j]$ :

$$\int_{I_j} f(t) dt \approx \sum_{\mu=1}^m w_\mu f(\tau_\mu), \quad \tau_\mu \in [t_{j-1}, t_j].$$

Define for  $1 \leq \mu \leq m$

$$M_\mu^{(t)} = [\eta_{s'}(\tau_\mu) \cdot \eta_s(\tau_\mu)]_{s,s'}, \quad T_\mu^{(t)} = [\eta_{s'}'(\tau_\mu) \cdot \eta_s(\tau_\mu)]_{s,s'},$$

$$C_\mu^{(t)} = [\eta_{s'}'(\tau_\mu) \cdot \eta_{s'}'(\tau_\mu)]_{s,s'}, \quad G^{(t)} = [\eta_{s'}(t_{j-1}) \cdot \eta_s(t_{j-1})]_{s,s'}$$

for  $0 \leq s, s' \leq r$  and

$$M_{\ell,\ell'}^{(r)} = [(\varphi_{\ell', \mathbf{k}'} \cdot \varphi_{\ell, \mathbf{k}})], \quad T_{\mu,\ell,\ell'}^{(r)} = [(\partial_{\beta(\tau_\mu, \cdot)} \varphi_{\ell', \mathbf{k}'}, \varphi_{\ell, \mathbf{k}})],$$

$$C_{\mu,\ell,\ell'}^{(r)} = [(\partial_{\beta(\tau_\mu, \cdot)} \varphi_{\ell', \mathbf{k}'}, \partial_{\beta(\tau_\mu, \cdot)} \varphi_{\ell, \mathbf{k}})], \quad K_{\mu,\ell,\ell'}^{(r)} = [(\sigma(\tau_\mu, \cdot) \varphi_{\ell', \mathbf{k}'}, \varphi_{\ell, \mathbf{k}})], \quad (15)$$

$$\tilde{K}_{\mu,\ell,\ell'}^{(r)} = [(\sigma(\tau_\mu, \cdot) \varphi_{\ell', \mathbf{k}'}, \partial_{\beta(\tau_\mu, \cdot)} \varphi_{\ell, \mathbf{k}})], \quad G_{\mu,\ell,\ell'}^{(r)} = [\langle \varphi_{\ell', \mathbf{k}'}, \varphi_{\ell, \mathbf{k}} \rangle_{\hat{\Gamma}_x^-(\tau_\mu)}]$$

with indices  $\mathbf{k} \leq n_\ell, \mathbf{k}' \leq n_{\ell'}$ . Hence one block can be approximated by

$$A_{\ell,\ell'}^{(\delta)} \approx \bar{A}_{\ell,\ell'}^{(\delta)}$$

$$= \sum_{\mu}^m w_\mu \left[ (T_\mu^{(t)} + \delta C_\mu^{(t)}) \otimes M_{\ell,\ell'}^{(r)} + \delta T_\mu^{(t)} \otimes (T_{\mu,\ell,\ell'}^{(r)})^T \right.$$

$$+ \delta (T_\mu^{(t)})^T \otimes (T_{\mu,\ell,\ell'}^{(r)} + K_{\mu,\ell,\ell'}^{(r)})$$

$$+ M_\mu^{(t)} \otimes (T_{\mu,\ell,\ell'}^{(r)} + \delta C_{\mu,\ell,\ell'}^{(r)} + K_{\mu,\ell,\ell'}^{(r)} + \tilde{K}_{\mu,\ell,\ell'}^{(r)} - G_{\mu,\ell,\ell'}^{(r)}) \left. \right]$$

$$+ G^{(t)} \otimes M_{\ell,\ell'}^{(r)}.$$

The matrix  $M_{\ell,\ell'}^{(\tau)}$  acting on the variables  $\mathbf{x}$  and  $\mathbf{v}$  has itself a tensor product structure

$$M_{\ell,\ell'}^{(\tau)} = M_{\ell_1,\ell'_1}^{(1)} \otimes M_{\ell_2,\ell'_2}^{(2)}, \quad M_{\ell,\ell'}^{(i)} = [(\boldsymbol{\varphi}_{\ell',k'}^{(i)}, \boldsymbol{\varphi}_{\ell,k}^{(i)})_{L^2(\Omega^{(i)})}]_{k,k'},$$

which can be exploited. In general this is not the case for the other matrices, making a  $2d$ -dimensional integration necessary. In the following we will therefore assume that the coefficients  $\beta$  and  $\sigma$  have a tensor product structure in the sense of

$$\begin{aligned} \beta(t, \mathbf{x}, \mathbf{v}) &= \sum_{i=1}^d a_i(t, \mathbf{x}) b_i(t, \mathbf{v}) \mathbf{e}_i + c_i(t, \mathbf{x}) d_i(t, \mathbf{v}) \mathbf{e}_{i+d}, \\ \sigma(t, \mathbf{x}, \mathbf{v}) &= p(t, \mathbf{x}) q(t, \mathbf{v}), \end{aligned}$$

where  $\mathbf{e}_i$  is the  $i$ -th unit vector, or can be represented (approximately) in a short sum of such tensor products. In the first case for example

$$\begin{aligned} T_{\mu,\ell,\ell'}^{(\tau)} &= \sum_{i=1}^d \left[ (a_i(\boldsymbol{\tau}_\mu, \cdot) \partial_{x_i} \boldsymbol{\varphi}_{\ell'_1,k'_1}^{(1)}, \boldsymbol{\varphi}_{\ell_1,k_1}^{(1)})_{L^2(\Omega^{(1)})} \cdot (b_i(\boldsymbol{\tau}_\mu, \cdot) \boldsymbol{\varphi}_{\ell'_2,k'_2}^{(2)}, \boldsymbol{\varphi}_{\ell_2,k_2}^{(2)})_{L^2(\Omega^{(2)})} \right]_{\mathbf{k},\mathbf{k}'} \\ &+ \sum_{i=1}^d \left[ (c_i(\boldsymbol{\tau}_\mu, \cdot) \boldsymbol{\varphi}_{\ell'_1,k'_1}^{(1)}, \boldsymbol{\varphi}_{\ell_1,k_1}^{(1)})_{L^2(\Omega^{(1)})} \cdot (d_i(\boldsymbol{\tau}_\mu, \cdot) \partial_{v_i} \boldsymbol{\varphi}_{\ell'_2,k'_2}^{(2)}, \boldsymbol{\varphi}_{\ell_2,k_2}^{(2)})_{L^2(\Omega^{(2)})} \right]_{\mathbf{k},\mathbf{k}'} \\ &= \sum_{i=1}^d (A_{i,\ell_1,\ell'_1}^{(\mu)} \otimes B_{i,\ell_2,\ell'_2}^{(\mu)} + C_{i,\ell_1,\ell'_1}^{(\mu)} \otimes D_{i,\ell_2,\ell'_2}^{(\mu)}) \end{aligned}$$

with appropriately defined matrices. The generalization to a short sum is straight forward. All other matrices can be treated analogously except the matrices  $G_{\mu,\ell,\ell'}^{(\tau)}$  for the boundary condition which in some cases may also be written in form of a tensor product, see the example in Sect 5.2.

Using this strategy, the calculation of the factors can be reduced to  $d$ -dimensional integrals over  $\Omega^{(i)}$ . Due to the multilevel structure of the spaces  $V_j^{(i)}$  it suffices to calculate the matrices on the finest scale and then use an interpolation operator. For  $\ell' < \ell$  denote by  $E_{\ell,\ell'}^{(i)}$  the matrix representation of the embedding from  $V_{\ell'}^{(i)}$  in  $V_\ell^{(i)}$ . Then for example

$$A_{i,\ell,\ell'}^{(\mu)} = (E_{L,\ell}^{(i)})^T \cdot A_{i,L,L}^{(\mu)} \cdot E_{L,\ell'}^{(i)}.$$

For the calculation of  $A_{i,L,L}^{(\mu)}$  classical finite element libraries can be used directly.

The application of the matrix  $A^{(\delta)}$  to a vector  $\mathbf{u}$  can be done blockwise, i.e. where block  $\ell$  is given by

$$[A^{(\delta)} \mathbf{u}]_\ell = \sum_{|\ell'|_1=L+1} A_{\ell,\ell'}^{(\delta)} \cdot \mathbf{u}_{\ell'}$$

while the tensor product structure can be exploited for each block. However the order of application is crucial [22,26] to prevent the need to store intermediate results on full grids. Therefore to calculate

$$S^{(t)} \otimes S_{\ell_1, \ell_1}^{(1)} \otimes S_{\ell_2, \ell_2}^{(2)} \mathbf{u}_{\ell'}$$

for general matrices  $S^{(t)}, S^{(1)}, S^{(2)}$  we will use

$$(S^{(t)} \otimes \text{Id}_{\ell_1}^{(1)} \otimes \text{Id}_{\ell_2}^{(2)}) \cdot (\text{Id}^{(t)} \otimes S_{\ell_1, \ell_1}^{(1)} \otimes \text{Id}_{\ell_2}^{(2)}) \cdot (\text{Id}^{(t)} \otimes \text{Id}_{\ell_1}^{(1)} \otimes S_{\ell_2, \ell_2}^{(2)}) \cdot \mathbf{u}_{\ell'}$$

in the case  $\ell'_1 + \ell_2 \leq \ell_1 + \ell'_2$  and

$$(S^{(t)} \otimes \text{Id}_{\ell_1}^{(1)} \otimes \text{Id}_{\ell_2}^{(2)}) \cdot (\text{Id}^{(t)} \otimes \text{Id}_{\ell_1}^{(1)} \otimes S_{\ell_2, \ell_2}^{(2)}) \cdot (\text{Id}^{(t)} \otimes S_{\ell_1, \ell_1}^{(1)} \otimes \text{Id}_{\ell_2}^{(2)}) \cdot \mathbf{u}_{\ell'}$$

otherwise, where  $\text{Id}$  the identity matrix in the respective spaces. The application of such a tensor product matrix can be applied in log-linear complexity with respect to the degrees of freedom.

### 4.3 Solution of Linear System of Equations

For the solution of (14) we will use an iterative method to exploit the tensor product structure of the block matrices. For a quite general class of symmetric bilinear form it can be shown that the combination technique alone, which combines the solution on anisotropic full grids has the same order of convergence as the sparse grid solution [8]. An alternative is to use these solutions as a preconditioner, see [24] in the case of radiative transfer.

In our non-symmetric case we will use the combination technique as a preconditioner for an outer Richardson iteration. More precisely starting with  $\mathbf{u}^{(0)} = 0$  we will calculate for  $k = 0, 1, \dots$

$$\mathbf{u}^{(k+1)} = \mathbf{u}^{(k)} - \Delta \mathbf{u}^{(k)}, \quad \Delta \mathbf{u}^{(k)} = P^{-1} \mathbf{r}^{(k)}, \quad \mathbf{r}^{(k)} = A^{(\delta)} \mathbf{u}^{(k)} - \mathbf{b}^{(\delta)}$$

until the norm of preconditioned residuum is small enough, i.e.  $\|\Delta \mathbf{u}^{(k)}\|_{L^2(J \times \Omega)} < \varepsilon$ , for some tolerance  $\varepsilon$ . Here  $P^{-1}$  denotes the application of the combination technique analog to [8], which will be described in the following.

To compute  $\Delta \mathbf{u}^{(k)}$  we solve

$$A_{\ell, \ell}^{(\delta)} \Delta \widehat{\mathbf{u}}_{\ell}^{(k)} = \mathbf{r}_{\ell}^{(k)} \tag{16}$$

for all  $\ell$  such that  $|\ell|_1 = L, L+1$ . For  $|\ell|_1 = L$  the residuum  $\mathbf{r}_{\ell}^{(k)}$  can be computed using the transpose of the embedding:

$$\mathbf{r}_{\ell_1-1, \ell_2}^{(k)} = (\text{Id}^{(t)} \otimes (E_{\ell_1, \ell_1-1}^{(i)})^T \otimes \text{Id}_{\ell_2}^{(2)}) \mathbf{r}_{\ell_1, \ell_2}^{(k)}, \quad \ell_1 > 1.$$

The system (16) has to be solved on small anisotropic full grid spaces. Currently now direct or iterative methods based on GMRES with an ILU preconditioner are used for this purpose, which require the computation of a matrix representation, however. For

the future it would be beneficial to overcome this requirement and devise schemes similar to [9] for the case of symmetric bilinear forms or use preconditioned iterative schemes for the anisotropic full grids [20].

We combine the results according to

$$\Delta \mathbf{u}^{(k)} = [\Delta \mathbf{u}_\ell^{(k)}]_\ell, \quad \Delta \mathbf{u}_\ell^{(k)} = \begin{cases} \Delta \hat{\mathbf{u}}_\ell^{(k)} & \ell_1 = 1 \\ \Delta \hat{\mathbf{u}}_\ell^{(k)} - (E_{\ell_1, \ell_1-1}^{(1)} \otimes \text{Id}_{\ell_2}^{(2)}) \Delta \hat{\mathbf{u}}_{\ell_1-1, \ell_2}^{(k)} & \ell_1 > 1 \end{cases}$$

Note that we used the embedding to represent the solution on spaces with level  $|\ell|_1 = L + 1$ . For interpolation such a scheme can be shown to give the exact result [6].

## 5 Numerical Experiments

In this section we present numerical examples to study the method described in Sect 4. The implementation is based on the finite element library MFEM [1] and uses its Python wrapper PyMFEM<sup>1</sup>. Due to the regular data structure of the combination technique standard numerical routines from `numpy`<sup>2</sup> and `scipy`<sup>3</sup> were used. The `cupy`<sup>4</sup> library was used as a replacement for the numerical libraries to perform the calculations on a GPU with only minor code changes. The computations were carried out on a desktop computer (i9 7900, 128 GB RAM, GTX 1080).

### 5.1 Linear advection with constant coefficients

As the first example we consider the linear advection equation with constant coefficients in  $d + d$  dimensions

$$\begin{aligned} \partial_t u + \mathbf{1} \cdot \nabla_{\mathbf{x}} u + \mathbf{1} \cdot \nabla_{\mathbf{v}} u &= 0, \quad \mathbf{x}, \mathbf{v} \in [0, 1]^d \\ u(0, \mathbf{x}, \mathbf{v}) &= \sin \left( 2\pi \sum_{i=1}^d (x_i + v_i) \right) \end{aligned} \quad (17)$$

with periodic boundary conditions. The solution is given by

$$u(t, \mathbf{x}, \mathbf{v}) = \sin \left( 2\pi \left( \sum_{i=1}^d (x_i + v_i) - 2dt \right) \right),$$

which is periodic in  $t$  for  $T = 1/(2d)$ .

The mesh on the coarsest scale on each  $\Omega^{(i)}$  consists of  $4^d$   $d$ -cubes of equal size and is uniformly refined for finer scales. The finite element functions are continuous piecewise polynomials of order  $r$  for  $r = 1, 2, 3$ . The streamline diffusion parameter is chosen as the edge length on the finest scale. The equation is solved on one period

<sup>1</sup> <https://github.com/mfem/PyMFEM>

<sup>2</sup> <https://numpy.org/>

<sup>3</sup> <https://scipy.org/>

<sup>4</sup> <https://cupy.dev/>

$L$	$h$	rel. err.	order	rel. err.	order	rel. err.	order
$d = 1$		$r = 1$		$r = 2$		$r = 3$	
1	2.50e-01	1.42e+00		1.75e-01		5.82e-03	
2	1.25e-01	6.26e-01	1.18	8.82e-03	4.31	4.01e-04	3.86
3	6.25e-02	1.27e-01	2.30	6.89e-04	3.68	2.67e-05	3.91
4	3.12e-02	2.27e-02	2.49	8.06e-05	3.10	1.70e-06	3.97
5	1.56e-02	4.63e-03	2.29	1.01e-05	3.00	1.06e-07	3.99
6	7.81e-03	1.09e-03	2.09	1.27e-06	2.99	6.67e-09	4.00
$d = 2$		$r = 1$		$r = 2$		$r = 3$	
1	2.50e-01	2.04e+00		2.71e-01		1.47e-02	
2	1.25e-01	9.51e-01	1.10	1.42e-02	4.26	5.86e-04	4.64
3	6.25e-02	2.36e-01	2.01	9.91e-04	3.84	4.47e-05	3.71
4	3.12e-02	4.86e-02	2.28	1.11e-04	3.15	2.54e-06	4.14
5	1.56e-02	1.14e-02	2.09	1.39e-05	3.00		
6	7.81e-03	3.00e-03	1.93	1.75e-06	2.99		
$d = 3$		$r = 1$		$r = 2$		$r = 3$	
1	2.50e-01	2.85e+00		3.61e-01			
2	1.25e-01	1.27e+00	1.17	2.00e-02	4.17		
3	6.25e-02	3.57e-01	1.82	1.22e-03	4.04		
4	3.12e-02	8.06e-02	2.15				
5	1.56e-02	1.65e-02	2.29				

**Table 1** Relative error with respect to the  $L_2$ -norm and estimated order of the numerical solution of (17) on  $d + d$  dimensions after one period for sparse grid spaces with levels  $L$  and order  $r$  of the ansatz functions;  $h$  denotes the grid size of the finest level

$T$  using discontinuous polynomials of the same order  $r$  as in the spatial discretization and  $2^{L+1}$  steps.

The final approximation at  $t = T$  is then refined on a sparse grid space of level  $L + 1$  and compared to the interpolation of the analytic solution. More precisely we compute the relative error with respect to the  $L^2$ -norm, i.e. the absolute error divided by the norm of the (interpolated) analytic solution. Table 1 reports the results, where the order is calculated from the errors of two successive runs. The convergence is also depicted in Fig. 1.

The order seems to scale like  $h^{r+1}$  independent of the dimension, one half bigger than the theoretical value from Thm 4.

## 5.2 L-shaped Spatial Domain

In the next example we solve the kinetic equation

$$\partial_t u + v \cdot \nabla_x u = 0, \quad [0, 1] \times \Omega \quad (18)$$

on a L-shaped spatial domain

$$\Omega = \Omega^{(1)} \times \Omega^{(2)}, \quad \Omega^{(1)} = (-1, 1)^2 \setminus [0, 1]^2, \quad \Omega^{(2)} = [-2, 0] \times [0, 2],$$

see Fig. 2. This demonstrates the use of the method for non-rectangular domains, boundary conditions, and discontinuous solutions. We choose zero inflow boundary



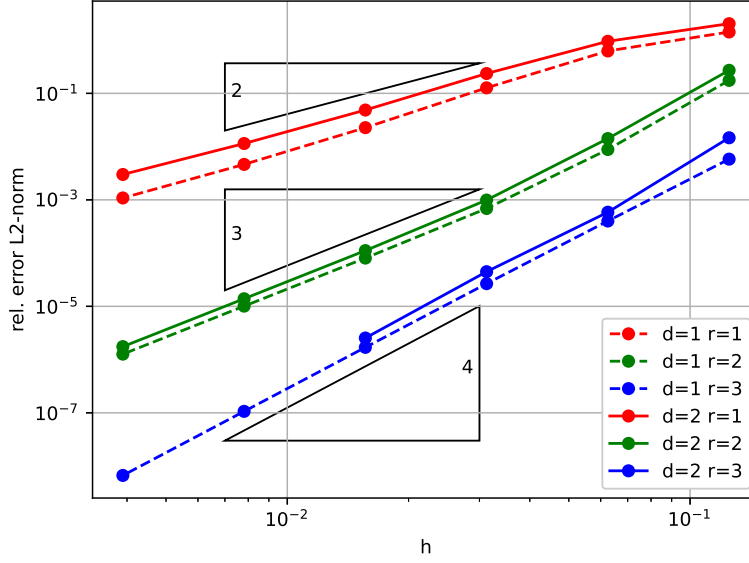


**Fig. 1** Relative error with respect to the  $L_2$ -norm of the numerical solution of (17) on  $d + d$  dimensions after one period for sparse grid spaces with order  $r$  of the ansatz functions;  $h$  denotes the grid size of the finest level

condition and

$$u_0(\mathbf{x}, \mathbf{v}) = \psi\left(\frac{x_1 - 0.5}{0.25}\right) \cdot \psi\left(\frac{x_2 + 0.5}{0.25}\right) \cdot \psi\left(\frac{v_1 + 1}{0.25}\right) \cdot \psi\left(\frac{v_2 - 1}{0.25}\right)$$

as the initial condition. Here  $\psi$  is a  $C^1$  function centered at 0 with width 1:

$$\psi(\xi) = \begin{cases} (|\xi| - 1)^2 \cdot (2|\xi| + 1) & |\xi| \leq 1 \\ 0 & |\xi| > 1 \end{cases}$$

For the assessment of the numerical results we will concentrate on the spatial distribution

$$\rho(t, \mathbf{x}) = \int_{\Omega^{(2)}} u(t, \mathbf{x}, \mathbf{v}) \, d\mathbf{v}. \quad (19)$$

The initial distribution  $u_0$  is supported in  $[0.25, 0.75] \times [-0.75, -0.25]$ . It is transported mainly in the direction  $[-1, 1]^T$  such that it is completely located in  $[-1, 0] \times [0, 1]$  at the final time  $t = 1$ , see Fig. 2. By the method of characteristics the solution is given by

$$u(1, \mathbf{x}, \mathbf{v}) = \begin{cases} u_0(\mathbf{x} - \mathbf{v}, \mathbf{v}) & v_1 x_2 > v_2 x_1 \\ 0 & \text{otherwise} \end{cases} \quad (20)$$

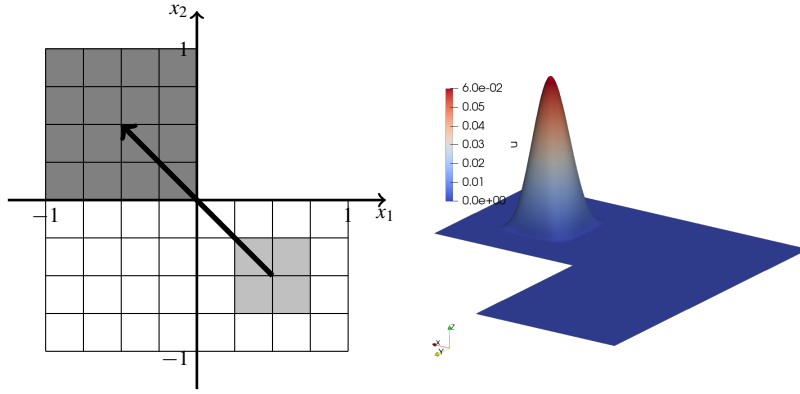


**Fig. 2** Left: spatial mesh on the coarsest scale for domain  $\Omega^{(1)}$ . The initial distribution is supported in the light gray area and is transported mainly along the arrow. It is completely contained in the dark area at  $t = 1$ ; right: initial spatial distribution  $\rho(0, \mathbf{x})$

for  $\mathbf{x} \in [-1, 0] \times [0, 1]$ ,  $\mathbf{v} \in [-1.25, -0.75] \times [0.75, 1.25]$ . Outside this domain it is zero. Here, the boundary leads to a discontinuous distribution.

The matrices  $G_{\mu, \ell, \ell'}^{(r)}$  from (15) corresponding to the boundary condition can be represented as a short sum of tensor products by partitioning the inflow boundary. For example the inflow at  $x_1 = -1$  with normal  $\mathbf{n} = [-1, 0, 0, 0]^T$  is given by

$$\{-1\} \times [-1, 1] \times \{\mathbf{v} \in \Omega^{(2)} \mid -v_1 < 0\}.$$

Hence its contribution to the element  $\mathbf{k}, \mathbf{k}'$  of  $G_{\mu, \ell, \ell'}^{(r)}$  can be calculated by

$$\int_{-1}^1 \int_{\Omega^{(2)}} \varphi_{\ell'_1, \mathbf{k}'_1}^{(1)}(-1, x_2) \cdot \varphi_{\ell_1, \mathbf{k}_1}^{(1)}(-1, x_2) \cdot \chi_{v_1 > 0}(\mathbf{v}) \cdot (-v_1) \cdot \varphi_{\ell'_2, \mathbf{k}'_2}^{(2)}(\mathbf{v}) \cdot \varphi_{\ell_2, \mathbf{k}_2}^{(2)}(\mathbf{v}) \, d\mathbf{v} \, dx_2$$

with the characteristic function  $\chi$ . This integral as well as the integrals over other sections of the inflow boundary can be factorized leading to a sum of tensor product operators for  $G_{\mu, \ell, \ell'}^{(r)}$ .

The coarsest mesh for the spatial domain  $\Omega^{(1)}$  is depicted in Fig. 2 and the domain  $\Omega^{(2)}$  is discretized by an  $8 \times 8$  regular grid. The equation is simulated for  $t \in [0, 1]$  with linear elements ( $r = 1$ ).

Fig. 3 (left) shows the resulting spatial distribution for  $t = 1$  and  $L = 5$ . In order to assess the numerical result it is compared to the distribution computed from the analytical solution (20) (right). The integration with respect to  $\mathbf{v}$  was carried out numerically. The results for levels up to  $L = 6$  are given in Table 2.

Although the solution  $u$  is discontinuous the numerical distribution  $\rho$  does not show oscillations thanks to the streamline diffusion. The theoretical results do not cover this case and it is too early to assess the order of convergence numerically. However the method seems to perform reasonable in this case.

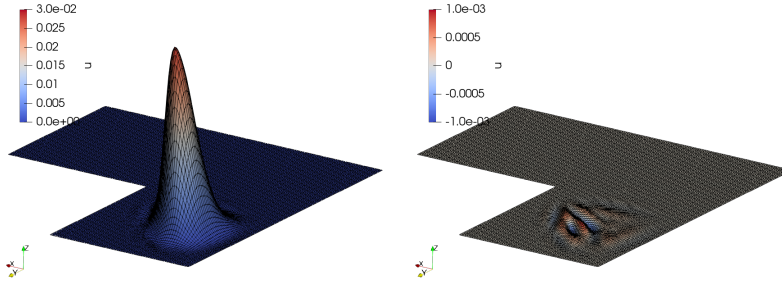


**Fig. 3** Left: Computed spatial distribution  $\rho(1, \mathbf{x})$  of (18) for  $L = 5$  and  $r = 1$ ; right: error of the computed spatial distribution

$L$	2	3	4	5	6
$h$	6.25e-02	3.12e-02	1.56e-02	7.81e-03	3.91e-03
rel. err.	5.89e-01	2.68e-01	6.56e-02	2.58e-02	1.28e-02
order		1.14	2.03	1.34	1.01

**Table 2** Relative error of the spatial distribution (19) with respect to the  $L_2$ -norm and estimated order of the numerical solution of (18) at  $t = 1$  for sparse grid spaces with levels  $L$  and linear elements;  $h$  denotes the grid size of the finest level

### 5.3 Vlasov-Poisson Equation

In plasma physics the particle density function  $f(t, \mathbf{x}, \mathbf{v})$  of electrons in a constant background ion density interacting with electrostatic fields ignoring collisions may be described by the Vlasov-Poisson equations

$$\partial_t f + \mathbf{v} \cdot \nabla_{\mathbf{x}} f - \mathbf{E}(f) \cdot \nabla_{\mathbf{v}} f = 0, \quad \nabla_{\mathbf{x}} \cdot \mathbf{E} = - \int f(t, \mathbf{x}, \mathbf{v}) d\mathbf{v} + 1, \quad \nabla \times \mathbf{E} = \mathbf{0}$$

supplemented by appropriate boundary conditions [5]. The first equation fits in the framework of the transport equation (1) except for the non-linearity due to the coupling with the electrical field. Nevertheless we may still use the method in a fixed-point iteration where the transport and field equation are solved alternately.

Given some approximation of the electrical field  $\mathbf{E}^{(k)}$  we may compute the density function  $f^{(k+1)}$  by solving

$$\partial_t f^{(k+1)} + \mathbf{v} \cdot \nabla_{\mathbf{x}} f^{(k+1)} - \mathbf{E}^{(k)}(t, \mathbf{x}) \cdot \nabla_{\mathbf{v}} f^{(k+1)} = 0. \quad (21)$$

using the method for linear transport equation presented here. Now given  $f^{(k+1)}$  we compute the resulting electrical field by solving the Poisson equation

$$-\Delta_{\mathbf{x}} \phi = - \int f^{(k+1)}(t, \mathbf{x}, \mathbf{v}) d\mathbf{v} + 1 \quad (22)$$

and letting  $\mathbf{E}^{(k+1)} = -\nabla_{\mathbf{x}} \phi$ .

Hence to solve the coupled equation in a time strip  $I_j = [t_{j-1}, t_j]$  we alternate the two steps. Starting with  $f^{(0)}$  as the final density  $f(t_{j-1}^-)$  of the last step and the resulting electrical field  $\mathbf{E}^{(0)}$  for all  $t \in I_j$  we iterate until

$$\|\mathbf{E}^{(k+1)} - \mathbf{E}^{(k)}\|_{L^2(I_j \times \Omega^{(1)})} + \|f^{(k+1)} - f^{(k)}\|_{L^2(I_j \times \Omega^{(1)} \times \Omega^{(2)})} < \varepsilon$$

for some tolerance  $\varepsilon$ .

Note that (22) has to be solved only at certain quadrature points  $\tau_\mu \in I_j$ , see Sect. 4.2, and that the integral of  $f$  on the right hand side can be represented by a finite element function on the finest grid of the space domain  $\Omega^{(1)}$ . Its solution is computed by the finite element method on the same grid. The order of the ansatz functions is increased by one leading to an exact solution. The preconditioner needed to solve (21) is updated if the rate of convergence decreases significantly.

As the first test we use the classic 1+1-dimensional Landau damping with initial condition

$$f(0, x, v) = f_0(x, v) = \frac{1}{\sqrt{2\pi}} e^{-v^2/2} (1 + \alpha \cos(kx))$$

and parameters  $\alpha = 10^{-2}$ ,  $k = 1/2$  on a periodic domain  $[0, 4\pi] \times [-v_{\max}, v_{\max}]$  with  $v_{\max}$  big enough [5]. We choose  $v_{\max} = 6$ .

We simulate the system in the time interval  $[0, 50]$ . On level  $L = 1$  each domain, i. e. space and velocity, is divided into four equally sized subintervals which are refined globally for higher levels. For  $L = 5$  one hundred times steps are performed, which are doubled for each increase in level. For the computation of the electrical field the midpoint rule is applied. A direct solver computes the resulting systems of linear equations for the transport as well as the potential equation.

Linear analysis shows that the electric field decays with a rate of  $\gamma \approx 0.153$  [19]. In Fig. 4 the electrical energy

$$\frac{1}{2} \int_{\Omega^{(1)}} \|\mathbf{E}(t, \mathbf{x})\|^2 d\mathbf{x}$$

exhibits the analytical decay rate up to  $t = 25$  or  $t = 30$  depending on the level  $L$ . Furthermore the invariants particle number, total energy and entropy, i.e.

$$\begin{aligned} \int_{\Omega} f(t, \mathbf{x}, \mathbf{v}) d\mathbf{x} d\mathbf{v}, \quad \frac{1}{2} \int_{\Omega} |\mathbf{v}|^2 f(t, \mathbf{x}, \mathbf{v}) d\mathbf{x} d\mathbf{v} + \frac{1}{2} \int_{\Omega^{(x)}} |\mathbf{E}(t, \mathbf{x})|^2 d\mathbf{x}, \\ \int_{\Omega} |f(t, \mathbf{x}, \mathbf{v})|^2 d\mathbf{x} d\mathbf{v} \end{aligned} \quad (23)$$

are shown. We see that the mass is almost conserved whereas the energy and entropy only up to a small error.

In the 2+2-dimensional setting we use  $\Omega = [0, 4\pi]^2 \times [-6, 6]^2$  and

$$f(0, \mathbf{x}, \mathbf{v}) = \frac{1}{2\pi} e^{-|\mathbf{v}|^2/2} (1 + \alpha \cos(kx_1) + \alpha \cos(kx_2)), \quad \alpha = 10^{-2}, k = \frac{1}{2}.$$

Again we simulate the system with the same settings as in the 1+1-dimensional case, where the coarsest meshes now consist of four by four squares. The results are shown in Fig 5. Qualitatively the results of the 1+1-dimensional setting are reproduced with slightly higher errors. Both tests show that the method can be used also in the case of nonlinear problems.

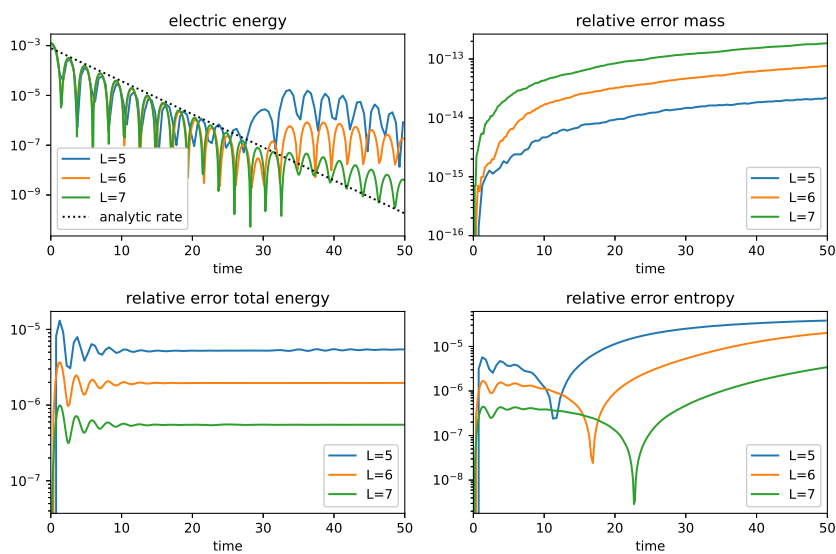


**Fig. 4** Simulation results of the 1+1-dimensional Landau damping for linear elements and different levels  $L$ ; the electric energy including the analytical decay rate and relative error of the invariants (23)

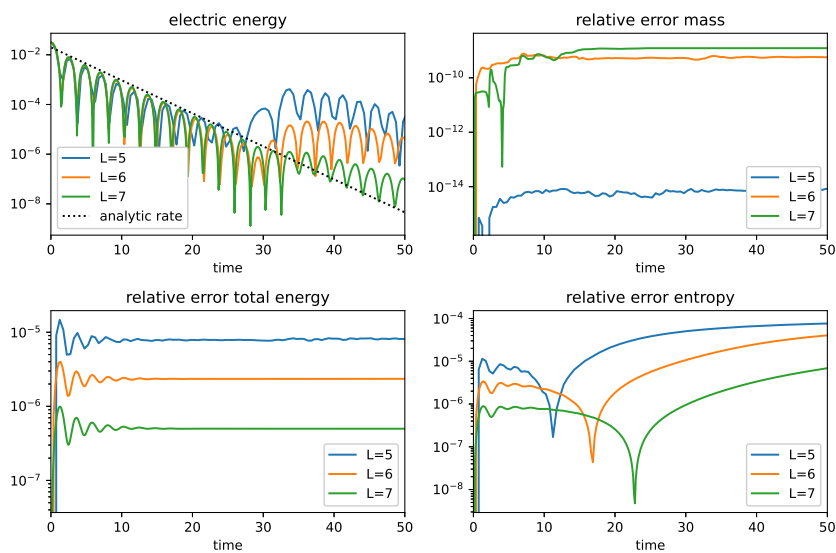


**Fig. 5** Simulation results of the 2+2-dimensional Landau damping for linear elements and different levels  $L$ ; the electric energy including the analytical decay rate and relative error of the invariants (23)

## 6 Outlook

In this paper we present a method which is capable of computing the solution of transport equations in moderately complex geometrical domains in up to 3+3-dimensional phase space. By using the sparse grid combination technique, traditional finite element libraries can be used. The resulting regular data structures facilitate parallelization and the use of GPU acceleration. By using a fixed-point iteration, this can also be used to compute the solution of nonlinear Vlasov-Poisson equations.

We aim to use the method for more complex geometries – for example, to simulate a plasma in an accelerator [16]. For such realistic problems it will be necessary to further parallelize the method. Again, the combination technique naturally leads to independent problems where each problem is a transport equation on anisotropic full grids which itself can be solved on multiple machines. It remains to further investigate efficient preconditioners for these systems.

The datasets generated during and analyzed in the current study are available from the corresponding author on reasonable request.

## Conflict of interest

The authors declare that no funds, grants, or other support were received during the preparation of this manuscript. The authors have no relevant financial or non-financial interests to disclose.

## References

1. Anderson, R., Andrej, J., Barker, A., Bramwell, J., Camier, J.S., Dobrev, J.C.V., Dudouit, Y., Fisher, A., Kolev, T., Pazner, W., Stowell, M., Tomov, V., Akkerman, I., Dahm, J., Medina, D., Zampini, S.: MFEM: A modular finite element methods library. *Computers & Mathematics with Applications* **81**, 42–74 (2021). DOI 10.1016/j.camwa.2020.06.009
2. Besse, N., Lattu, G., Ghizzo, A., Sonnendrücker, E., Bertrand, P.: A wavelet-MRA-based adaptive semi-Lagrangian method for the relativistic Vlasov–Maxwell system. *J. Comput. Phys.* **227**(16), 7889–7916 (2008). DOI 10.1016/j.jcp.2008.04.031
3. Bungartz, H.J., Griebel, M.: Sparse grids. *Acta Numerica* **13**, 147–269 (2004). DOI 10.1017/S0962492904000182
4. Deriaz, E., Peirani, S.: Six-Dimensional Adaptive Simulation of the Vlasov Equations Using a Hierarchical Basis. *Multiscale Modeling & Simulation* **16**(2), 583–614 (2018). DOI 10.1137/16M1108649
5. Einkemmer, L., Lubich, C.: A Low-Rank Projector-Splitting Integrator for the Vlasov–Poisson Equation. *SIAM J. Sci. Comput.* **40**(5), B1330–B1360 (2018). DOI 10.1137/18M116383X
6. Garcke, J.: Sparse Grids in a Nutshell. In: J. Garcke, M. Griebel (eds.) *Sparse Grids and Applications*, vol. 88, pp. 57–80. Springer, Berlin, Heidelberg (2012). DOI 10.1007/978-3-642-31703-3\_3
7. Griebel, M., Harbrecht, H.: On the construction of sparse tensor product spaces. *Math. Comput.* **82**, 975–994 (2013). DOI 10.1090/S0025-5718-2012-02638-X
8. Griebel, M., Harbrecht, H.: On the Convergence of the Combination Technique. In: J. Garcke, D. Pflüger (eds.) *Sparse Grids and Applications - Munich 2012, Lecture Notes in Computational Science and Engineering*, pp. 55–74. Springer International Publishing, Cham (2014). DOI 10.1007/978-3-319-04537-5\_3
9. Griebel, M., Hullmann, A.: On a Multilevel Preconditioner and its Condition Numbers for the Discretized Laplacian on Full and Sparse Grids in Higher Dimensions. In: *Singular Phenomena and Scaling in Mathematical Models*, pp. 263–296. Springer, Cham (2014). DOI 10.1007/978-3-319-00786-1\_12

10. Griebel, M., Knapek, S.: Optimized Tensor-Product Approximation Spaces. *Constructive Approximation* **16**(4), 525–540 (2000). DOI 10.1007/s003650010010
11. Griebel, M., Schneider, M., Zenger, C.: A combination technique for the solution of sparse grid problems. In: P. de Groen, R. Beauwens (eds.) *Iterative Methods in Linear Algebra*, pp. 263–281. IMACS, Elsevier, North Holland (1992)
12. Guo, W., Cheng, Y.: A Sparse Grid Discontinuous Galerkin Method for High-Dimensional Transport Equations and Its Application to Kinetic Simulations. *SIAM J. Sci. Comput.* **38**(6), A3381–A3409 (2016). DOI 10.1137/16M1060017
13. Harbrecht, H., Schneider, R., Schwab, C.: Multilevel frames for sparse tensor product spaces. *Numerische Mathematik* **110**(2), 199–220 (2008). DOI 10.1007/s00211-008-0162-x
14. Hilber, N.W.: *Stabilized Wavelet Methods for Option Pricing in High Dimensional Stochastic Volatility Models*. Ph.D. thesis, ETH Zürich (2009)
15. Johnson, C., Nävert, U., Pitkäranta, J.: Finite element methods for linear hyperbolic problems. *Comput. Methods Appl. Mech. Eng.* **45**, 285–312 (1984). DOI 10.1016/0045-7825(84)90158-0
16. Keßler, T., Rjasanow, S., Weißer, S.: Vlasov-Poisson system tackled by particle simulation utilising boundary element methods. *SIAM J. Sci. Comput.* **42**(1), B299–B326 (2020). DOI 10.1137/18M1225823
17. Kormann, K., Sonnendrücker, E.: Sparse Grids for the Vlasov–Poisson Equation. In: *Sparse Grids and Applications - Stuttgart 2014, Lecture Notes in Computational Science and Engineering*, pp. 163–190. Springer, Cham (2016). DOI 10.1007/978-3-319-28262-6\_7
18. Larsson, S., Thomée, V.: *Partial Differential Equations with Numerical Methods*, corrected 2nd printing edn. No. 43 in *Texts in Applied Mathematics*. Springer, Berlin ; New York (2005)
19. Pham, N., Helluy, P., Crestetto, A.: Space-only hyperbolic approximation of the Vlasov equation. *ESAIM: Proceedings* **43**, 17–36 (2013). DOI 10.1051/proc/201343002
20. Reisinger, C., Wittum, G.: On multigrid for anisotropic equations and variational inequalities “Pricing multi-dimensional European and American options”. *Computing and Visualization in Science* **7**(3), 189–197 (2004). DOI 10.1007/s00791-004-0149-9
21. Schwab, C., Süli, E., Todor, R.A.: Sparse finite element approximation of high-dimensional transport-dominated diffusion problems. *ESAIM: Mathematical Modelling and Numerical Analysis* **42**(5), 777–819 (2008). DOI 10.1051/m2an:2008027
22. Schwab, C., Todor, R.A.: Sparse finite elements for elliptic problems with stochastic loading. *Numerische Mathematik* **95**(4), 707–734 (2003). DOI 10.1007/s00211-003-0455-z
23. Verboncoeur, J.P.: Particle simulation of plasmas: Review and advances. *Plasma Phys. Controlled Fusion* **47**, A231–A260 (2005). DOI 10.1088/0741-3335/47/5A/017
24. Widmer, G.: An Efficient Sparse Finite Element Solver for the Radiative Transfer Equation. *J. Heat Transfer* **132**(2) (2009). DOI 10.1115/1.4000190
25. Widmer, G., Hiptmair, R., Schwab, C.: Sparse adaptive finite elements for radiative transfer. *J. Comput. Phys.* **227**(12), 6071–6105 (2008). DOI 10.1016/j.jcp.2008.02.025
26. Zeiser, A.: Fast Matrix-Vector Multiplication in the Sparse-Grid Galerkin Method. *J. Sci. Comput.* **47**(3), 328–346 (2011). DOI 10.1007/s10915-010-9438-2